Piezoelectrically Actuated Flextensional Micromachined Ultrasound Transducers—II: Fabrication and Experiments

Gökhan Perçin, *Member, IEEE*, and Butrus T. Khuri-Yakub, *Fellow, IEEE*

***Abstract*—This paper presents novel micromachined two-dimensional array piezoelectrically actuated flextensional transducers that can be used to generate sound in air or water. Micromachining techniques to fabricate these devices are also presented. Individual unimorph array elements consist of a thin piezoelectric annular disk and a thin, fully clamped, circular plate. We manufacture the transducer in two-dimensional arrays using planar silicon micromachining and demonstrate ultrasound transmission in air at 2.85 MHz with 0.15 μm/V peak displacement. The devices have a range of operating resonance frequencies starting from 450 kHz to 4.5 MHz. Such an array could be combined with on-board driving and addressing circuitry for different applications.**

I. Introduction

TWO-DIMENSIONAL arrays of ultrasound transducers are desirable for imaging applications in the fields of medicine, nondestructive evaluation, and underwater exploration. Making arrays of transducers by dicing and connecting individual piezoelectric elements is fraught with difficulty and expense, not to mention the large input impedance mismatch problem that such elements present to transmit/receive electronics. Our approach is to use micromachined flextensional unimorph piezoelectric transducers. Individual elements are made of thin silicon nitride plates covered by a coating of piezoelectric ZnO. The arrays are made by using silicon micromachining techniques and are capable of operation at high frequencies as well as at low frequencies. Inherently, this approach offers the advantage of integrating transducers with transmitter and receiver electronics. Thus, we present arrays in which elements can be individually addressed for ease of scanning and focusing by using on-board electronics.

Flextensional unimorph piezoelectric transducers can be used both for reception and for radiation. The utility of this type of transducer lies primarily in its ability to generate electrical signals from mechanical and acoustical sources of low impedance and to develop relatively large motions (and low force) with modest electrical excitation. As for the generation of sound waves, matching between the mechanical impedance of the transducer and the radiation impedance should be taken into account. The series connections of these transducers develop twice the voltage of the parallel connections for the same driving force, but provide only one-half of the displacement of parallel connections for the same applied voltage. The electrical impedance of the series connections is four times the impedance of the parallel connections. Their high sensitivity, large displacement to voltage ratio and large electrical capacitance combined with small dimensions and a large range of operating resonance frequencies cannot be realized by any other kind of ultrasonic transducer, i.e., longitudinal mode piezoelectric transducer and capacitive transducer. To date, however, flextensional transducers have not been used in ultrasonic applications because of their low frequency response. Here, we present novel micromachined two-dimensional array flextensional unimorph ultrasonic tranducers that have typical operating resonance frequencies starting from 450 kHz to 4.5 MHz in air.

We fabricated micromachined piezoelectrically actuated flextensional transducers in a two-dimensional array by combining conventional integrated circuit (IC) manufacturing process technology with ZnO deposition. Individual array elements consist mainly of a circular plate attached to an annular disk of piezoelectric material that has optimized dimensions. An ac voltage is applied across the piezoelectric material to set the compound plate into vibration. At the resonant frequencies of the compound plate, the displacement at the center is large. A dc voltage together with an ac voltage applied to the piezoelectric can be used to fine tune the resonance of the compound plate. Because, the dc voltage effectively changes the stiffness of the plate by introducing a dc strain to the plate. Similar ultrasound transducer designs can be found in Bernstein [1], [2] and Takeuchi [3].

II. Design Parameters

General information about designing unimorph and bimorph transducers and reviews of theoretical models can be found in Germano [4] and Denkmann *et al.* [5]. The individual array element is designed to have a maximum volume displacement of the plate at the resonant frequency.

Manuscript received April 23, 2001; accepted November 12, 2001. This research was supported by the Defense Advanced Research Projects Agency of the Department of Defense and was monitored by the Air Force Office of Scientific Research under Grant No. F49620-95-1-0525. This work made use of the National Nanofabrication Users Network facilities funded by the National Science Foundation under award number ECS-9731294.

G. Perçin is with ADEPTIENT, Los Altos, CA 94024 (e-mail: percin@adeptient.com)

B. T. Khuri-Yakub is with Edward L. Ginzton Laboratory, Stanford University, Stanford, CA 94305-4085.

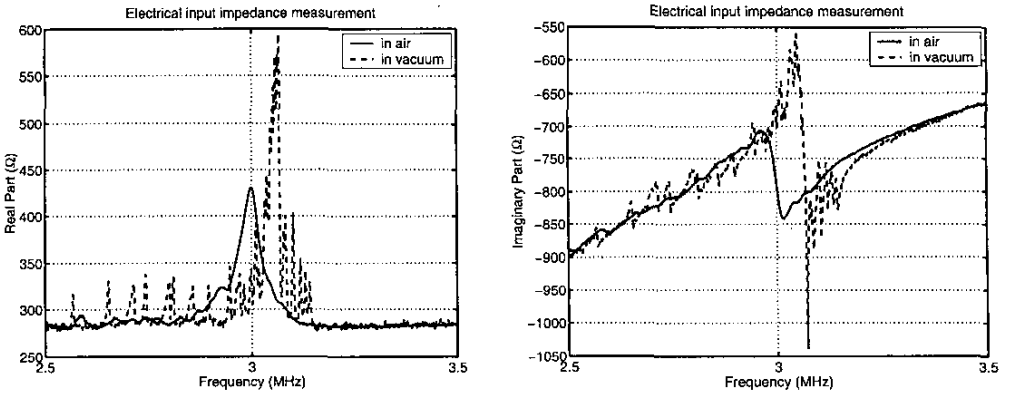

Fig. 1. Type I micromachined flextensional transducer measurements (Device A; 60 elements are connected).

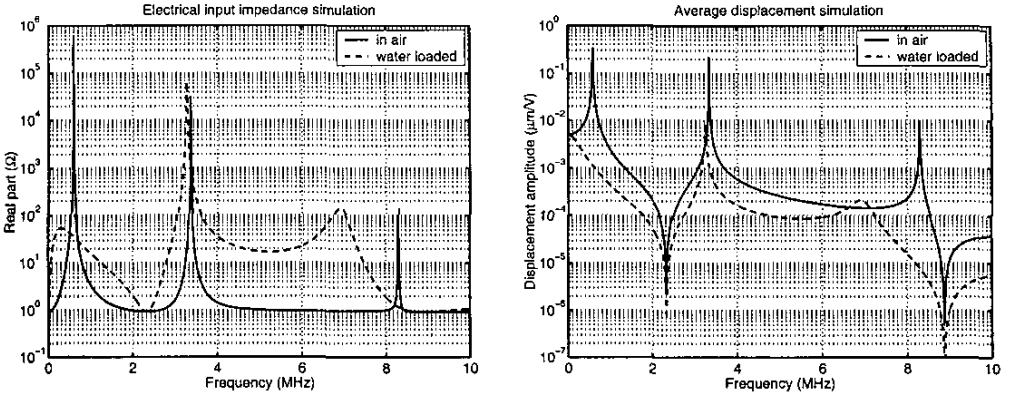

Fig. 2. Type I micromachined flextensional transducer simulations for a single element (Devices A, B, and C).

Analyses of similar devices such as those of Germano [4], Denkmann *et al.* [5], Allaverdiev *et al.* [6], Vassergiser *et al.* [7], Antonyak *et al.* [8], Brailov *et al.* [9], Adelman *et al.* [10], Okada *et al.* [11], Aronov *et al.* [12], [13], Rosato [14], Greenberg *et al.* [15], Stavsky *et al.* [16], and Rudgers [17] are helpful in identifying the important parameters of the device. However, the complexity of the structure and the fact that the piezoelectric used is an annular disk rather than a full disk necessitate the use of more complicated analyses to determine the resonant frequencies of the structure, the input impedance of the transducer, and the normal displacement of the surface. Indeed, the complete analysis of the transducer is presented in Perçin *et al.* [18].

We designed micromachined two-dimensional array transducers learning from the model of a one-element, large-scale prototype [19], [20]. However, the two-dimensional array nature of the device is accomodated by a suitable micromachining process [21]. Materials are chosen in accordance with availability of micromachining and IC manufacturing processes. Other piezoelectric materials, non-piezoelectric carrier plate materials, electrode metals, and substrates can be used.

Initially, a commercial finite element code, ANSYS, was used to optimize an individual array element made with piezoelectric ZnO on a silicon nitride plate. Several iterations were run to maximize the displacement of the plate as a function of the dimensions of the piezoelectric annular disk. Maximum displacement was obtained when the piezoelectric annular disk had an inner diameter of 30 μm and an outer diameter of 80 μm with a thickness of 0.3 μm, and the silicon nitride had a diameter of 100 μm with a thickness of 0.3 μm. The dc displacement is 2.27 Å/V. The resonance frequency (3.46 MHz) obtained from the ANSYS simulation in vacuum is in good agreement with the 3.07 MHz that was measured in vacuum with one of our devices as shown in Fig. 1. The details of the ANSYS simulation were presented in Perçin *et al.* [22]. By using the model developed in Perçin *et al.* [18], these results are confirmed as shown in Fig. 2. Fig. 2 also presents the electrical input impedance and average displacement of the individual array element for air- and water-loaded cases. The model developed can be used to compare conventional longitudinal mode transducer with the flexural mode transducer developed as shown in Table I. The displacement per volt and pressure per volt are important parameters for evaluating the performance of transmitter transducer. As seen in Table I, the displacement per volt and pressure per volt for the flexural mode transducer have considerably higher values compared with the conventional

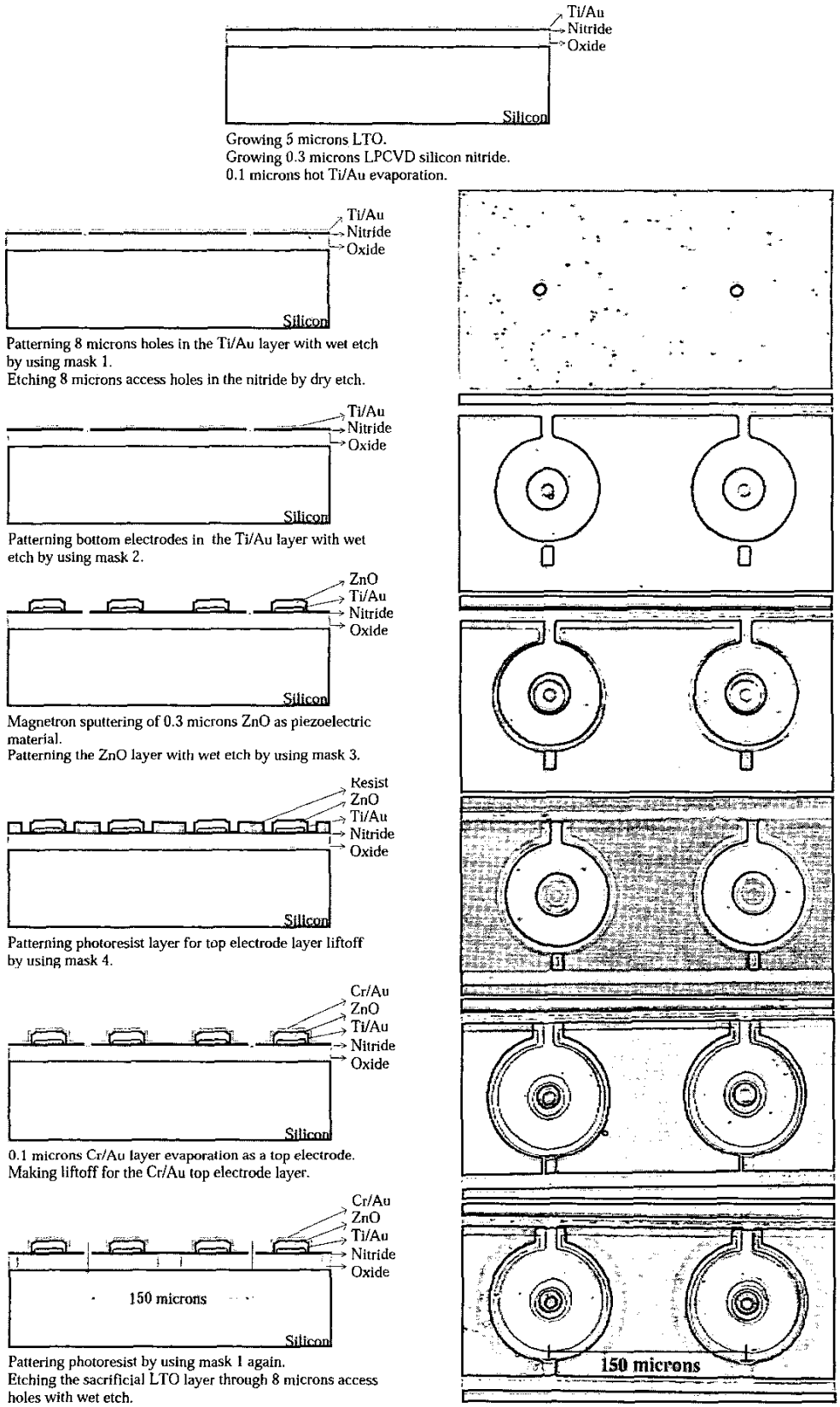

Fig. 3. Realized Type I micromachined device fabrication process flow.

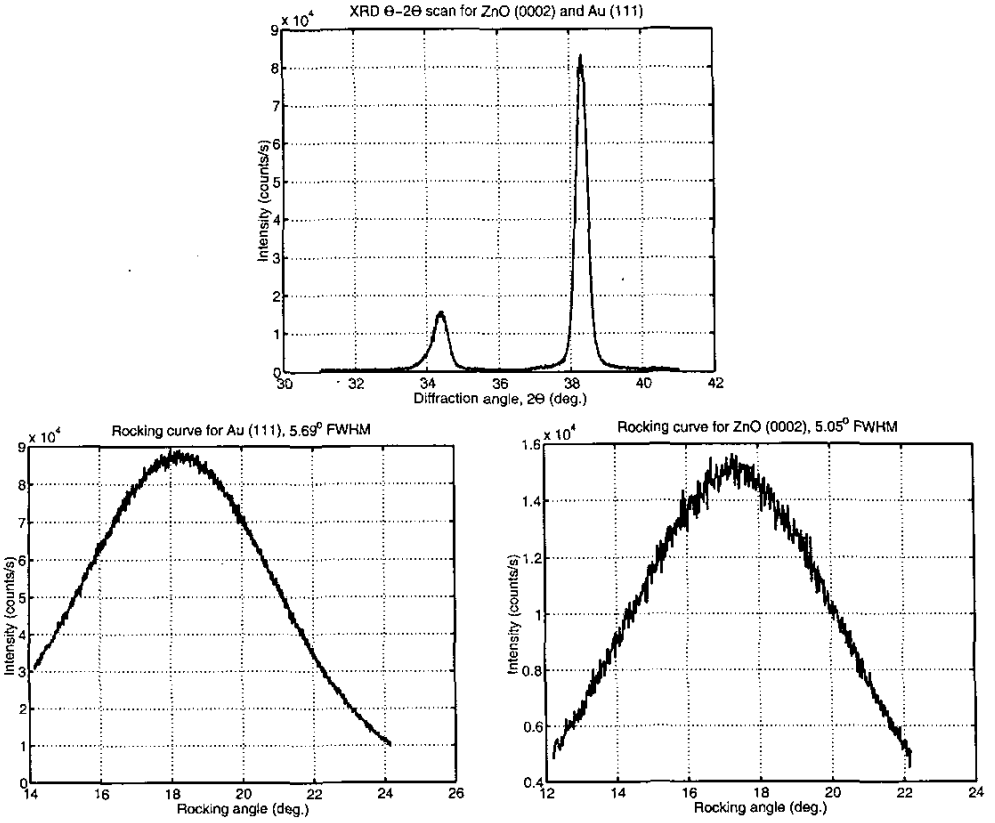

Fig. 4. X-ray diffraction measurements of ZnO (0002) and Au (111) films.

TABLE I

FLEXTENSIONAL VS. THICKNESS MODE TRANSDUCERS. (DEVICE E IS FLEXTENSIONAL.)

	Longitudinal mode transducer			Flexural mode transducer		
Piezoclectric material	PZT 5H Vernitron			Zinc oxide		
Relative permittivity	1470			11.1		
Transducer area (mm^2)	0.0104			0.0104		
Piezoelectric thickness (μm)	6350	1310	488	0.4		
Capacitance (zero strain, pF)	0.02	0.10	0.28	2.56		
Frequency (MHz)	0.320	1.55	4.17	0.320	1.55	4.17
Displacement/volt (in air, nm/V)	81	17	6.5	370	160	320
Pressure/volt (in air, Pa/V)	68	70	70	303	645	3478
Volt/pressure (in air, 50 Ω, nV/Pa)	87	88	87	380	810	4300
v/V when $P = 0$ (m/s/V)	0.17	0.17	0.17	1.3	8.3	16.4

TABLE II

PHYSICAL DIMENSIONS OF THE MICROMACHINED DEVICES.

Dimension (μm)	Devices A, B, C	Device D	Device E
Radius of the orifice	4.3	3.0	2.5
Inner radius of the piezoelectric layer	12.0	10.2	12.0
Outer radius of the piezoelectric layer	41.3	45.5	46.2
Radius of the device	45.0	58.7	57.5
Thickness of the carrier plate	0.30	0.25	0.25
Thickness of the piezoelectric layer	0.35	0.40	0.40
Thickness of the electrode layers	0.10	0.10	0.10

TABLE III
TYPE I MICROMACHINED FLEXTENSIONAL TRANSDUCER INTERFEROMETER MEASUREMENTS (DEVICE B).

Frequency MHz	Displacement μm/V
0.75	0.0053
1.25	0.0070
2.30	0.0090
2.90	0.1500
3.52	0.0175

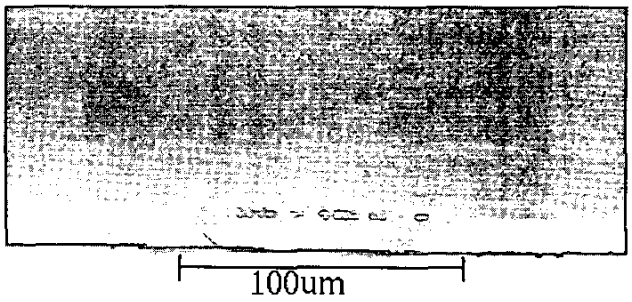

Fig. 6. Sideview of Type I micromachined device array element.

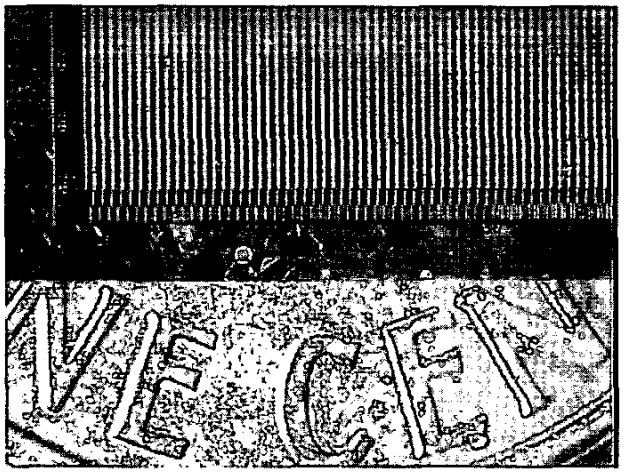

Fig. 5. Realized micromachined device.

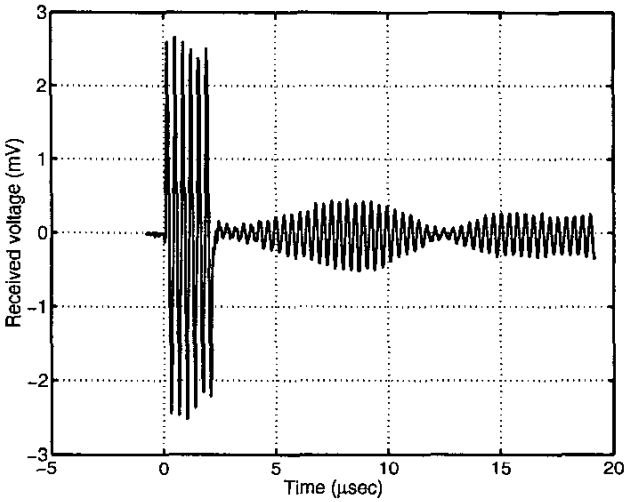

Fig. 7. Type I micromachined flextensional transducer air transmit/receive measurements (Devices A and C).

longitudinal mode transducer. The previous statement is also true for the volt-per-pressure parameter, which becomes important for evaluating the performance of a receiver transducer. The physical dimensions of the devices mentioned in this paper are shown in Table II.

III. DEVICE FABRICATION

The fabrication process for Type I micromachined two-dimensional array flextensional transducers is given in Fig. 3. At the right side of the figure, actual pictures of two adjacent elements from a two-dimensional array are given along with the process flow. The process starts with growing a sacrificial layer, chosen to be silicon oxide [8% phosphorus doped densified low temperature oxide (LTO)]. A non-piezoelectric carrier plate layer of low pressure chemical vapor deposition (LPCVD) silicon nitride is grown on top of the sacrificial layer. The bottom Ti/Au electrode layer is deposited on the non-piezoelectric carrier plate by e-beam evaporation at 228°C. The degree to which the ZnO c-axis, $< 002 >$ is oriented normal to the substrate surface is very sensitive to the degree to which the Au film is $< 111 >$ oriented. The quality of the ZnO is measured by an X-ray rocking curve scan. The ZnO had a 5.5°-wide rocking curve above Au with a 5°-wide rocking curve as shown in Fig. 4. The bottom metal layer is patterned by wet etch, and access holes for sacrificial layer etching are drilled in the non-piezoelectric carrier plate layer by plasma etching. Later, the bottom electrode layer is patterned by wet etch, and a piezoelectric ZnO layer is deposited on top of the bottom electrode. The ZnO is deposited by dc planar magnetron sputtering from a 127-mm wide target consisting of 99.99% Zn. The deposition is made in an 20 to 80% argon-oxygen ambient with a flow rate of 26.6 sccm, a pressure of 7 mTorr, a substrate temperature of 145°C, and a dc power of 350 W. The separation between the substrate and the target is 51 mm. The deposition rate is 9.0 Å/s. The top Cr/Au electrode layer is formed by e-beam evaporation at room temperature and patterned by liftoff. The last step is etching the sacrificial layer by wet etch, and this concludes the front surface micromachining of the devices. Fig. 5 shows final 60 × 60 two-dimensional array devices. The die size is 1 cm × 1 cm. Fig. 6 shows a sideview of the fabricated array element. The fabrication process for Type II micromachined two-dimensional array flextensional transducers and droplet ejectors is given in Perçin *et al.* [23].

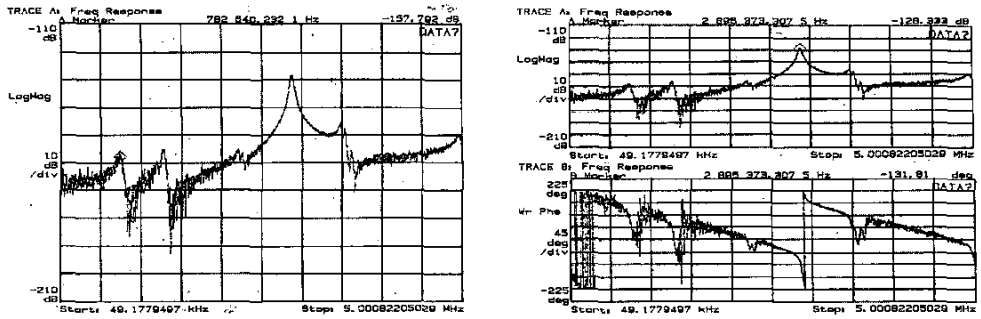

Fig. 8. Type I micromachined flextensional transducer interferometer measurements (Device B).

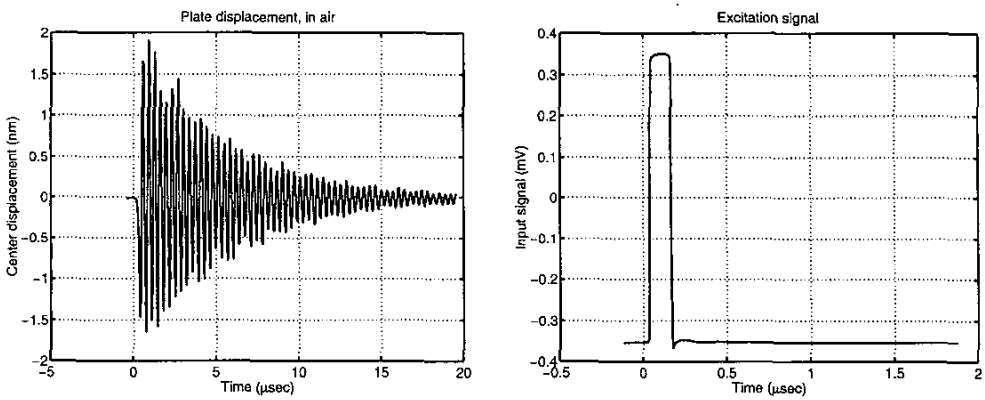

Fig. 9. Type I micromachined flextensional transducer interferometer measurements (Device B).

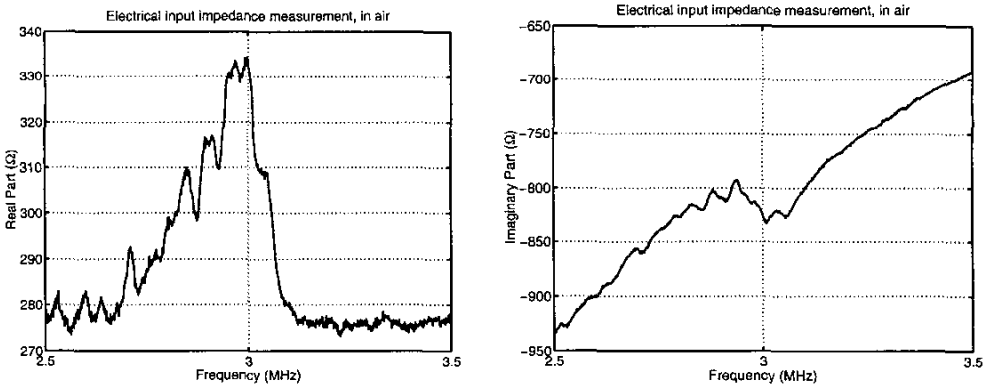

Fig. 10. Type I micromachined flextensional transducer measurements (Device B; 60 elements are connected).

IV. Experiments and Results

Fig. 1 shows the real part of the electrical input impedance of only one row of 60 elements of the devices shown in Fig. 5. Operating in air, the transducers have a resonant frequency of 3.0 MHz and a fractional bandwidth of about 1.5%. The real part of the electrical input impedance has a 280-Ω base value, and it was determined by SPICE simulation that this base value is caused by the bias lines connecting individual array elements. This can be avoided by using electroplating to increase the thickness of the bias lines. Fig. 1 also shows the existence of acoustical activity in the device and an acoustic radiation resistance R_a of 150 Ω. Fig. 1 presents the change of the electrical input impedance in vacuum of a device consisting of one row of 60 elements. The resonance frequency is 3.00 MHz in air and 3.07 MHz in vacuum (at 50 mTorr). This result is in accordance with our expectations, because the resonant frequency and the real part of electrical input impedance at resonance should increase in vacuum. The acoustic activity in vacuum reflects energy coupling to the structure. This is a major source of loss in

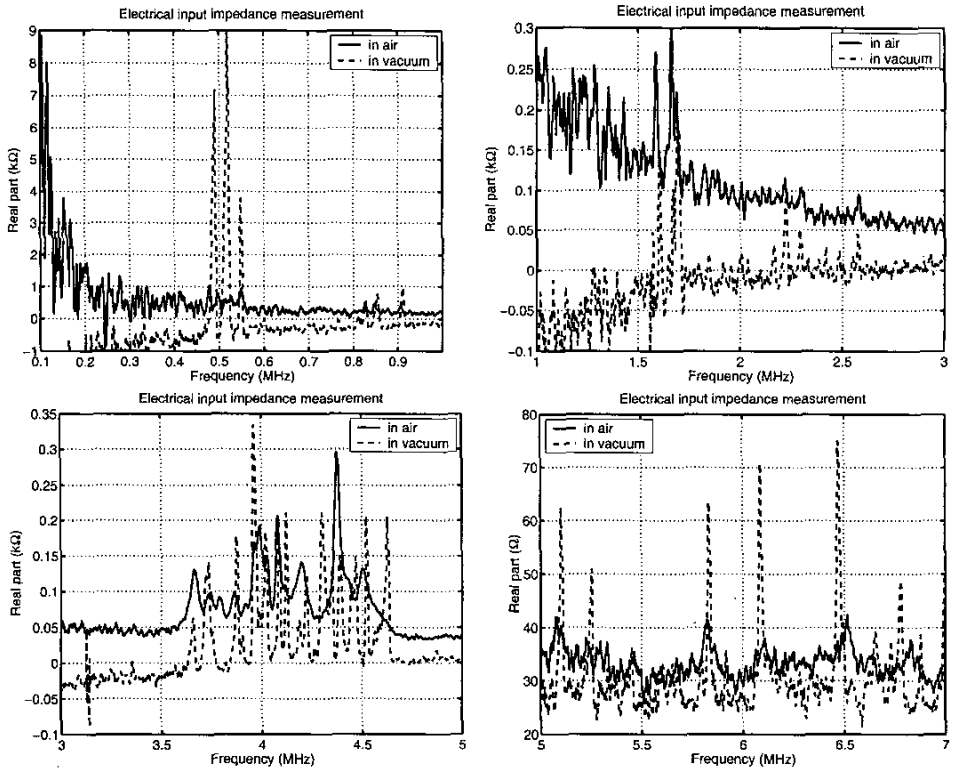

Fig. 11. Type II micromachined flextensional transducer measurements (Device D; three elements are connected).

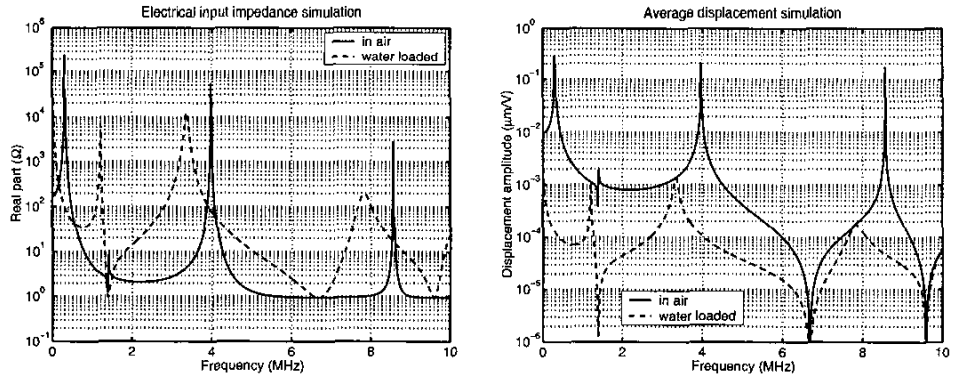

Fig. 12. Type II micromachined flextensional transducer simulations for a single element (Device D).

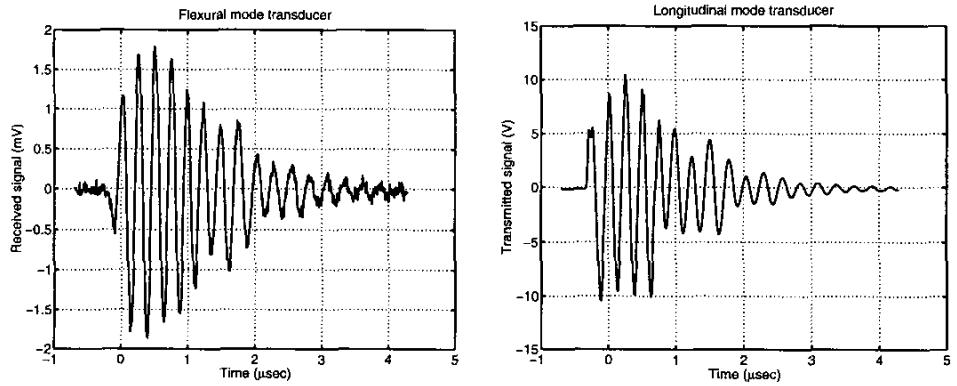

Fig. 13. Water-loaded Type II micromachined flextensional transducer measurements (Device E; four elements are connected).

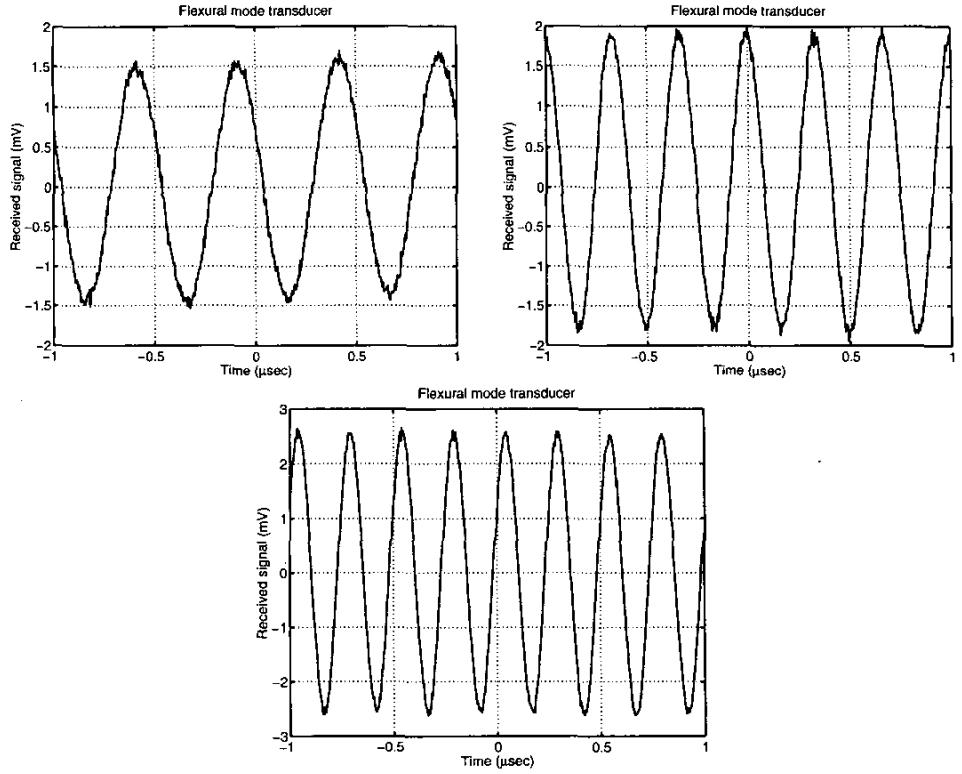

Fig. 14. Water-loaded Type II micromachined flextensional transducer measurements (Device E; four elements are connected).

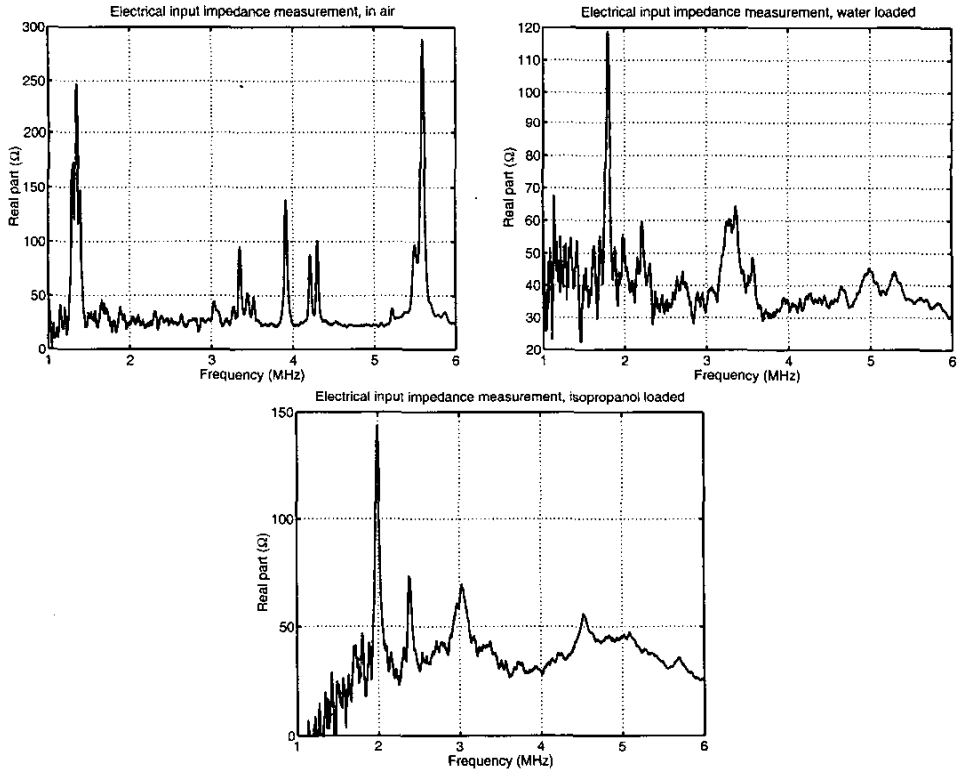

Fig. 15. Type II micromachined flextensional transducer measurements (Device E; four elements are connected).

the device and is a present topic of research in our group. Fig. 7 shows the result of an air transmission experiment in which an acoustic signal is received following the electromagnetic feedthrough. The insertion loss is 112 dB. In the transmit/receive experiment, the receiver had one row of 60 elements (Device A shown in Fig. 1), and the transmitter had two rows of 120 elements. Loss caused by eletrical mismatches is 34.6 dB. Other important loss sources are alignment of receiver and transmitter, diffraction, and structural losses.

Fig. 8 and 9 show compound plate displacement measurements using an optical interferometer. In Fig. 8, 0 dB corresponds to 0.5 m/V, and the device has a diameter of 90 μm. Electrical input impedance measurement of the device is given in Fig. 10. In Table III, the displacement values at different frequencies are shown. The highest peak displacement, 0.15 μm/V at 2.9 MHz, was obtained by scaling from 0.003 μm per 0.02-V input signal. The same device was also loaded by corn oil from both sides, and 1.2 nm/V peak displacement was obtained at 900 kHz. Fig. 8 also presents the relative phase of the plate displacement. In another experiment, the same device was excited by a short square wave shown in Fig. 9, and the plate displacement shown again in Fig. 9 was obtained. As shown in Fig. 9, the device has a high quality factor when operating in air.

Although the fabrication process for the Type II micromachined flextensional transducers and droplet ejectors is given in Perçin *et al.* [23], the electrical measurements and the simulation results of Type II devices are given here. There are not many differences between Type I and Type II devices; however, Type II devices include 100 μm-diameter thru-wafer fluid reservoirs that can also be used as an impedance matching back port load for transducer applications. In Fig. 11, the real parts of the electrical input impedance of the device in air and in vacuum are given. The device has three array elements connected in parallel. By using the electrical input impedance measurement in vacuum, the resonances of the device have been distinguished easily, and the model developed in Perçin *et al.* [18] was confirmed as shown in Fig. 12. By using another Type II device that has four array elements connected in parallel, 100-μm diameter thru-wafer fluid reservoirs were filled with water, and a conventional longitudinal thickness mode transducer was used to excite ultrasound waves in air at 4 MHz. The longitudinal mode transducer was driven with a sinusoidal tone burst with four cycles at 4 MHz. In Fig. 13, the received signal at the Type II transducer and the transmitted signal at the longitudinal mode transducer are shown. As seen in Fig. 13, the Type II device has a fractional bandwidth of 10% when loaded with water. The same Type II device and the longitudinal mode transducer were used to repeat the previous measurements with continuous sinusoidal signals at 2, 3, and 4 MHz as shown in Fig. 14. Fig. 13 and 14 demonstrate the acoustical or, equivalently, electromechanical activity in the devices when they are loaded with fluid.

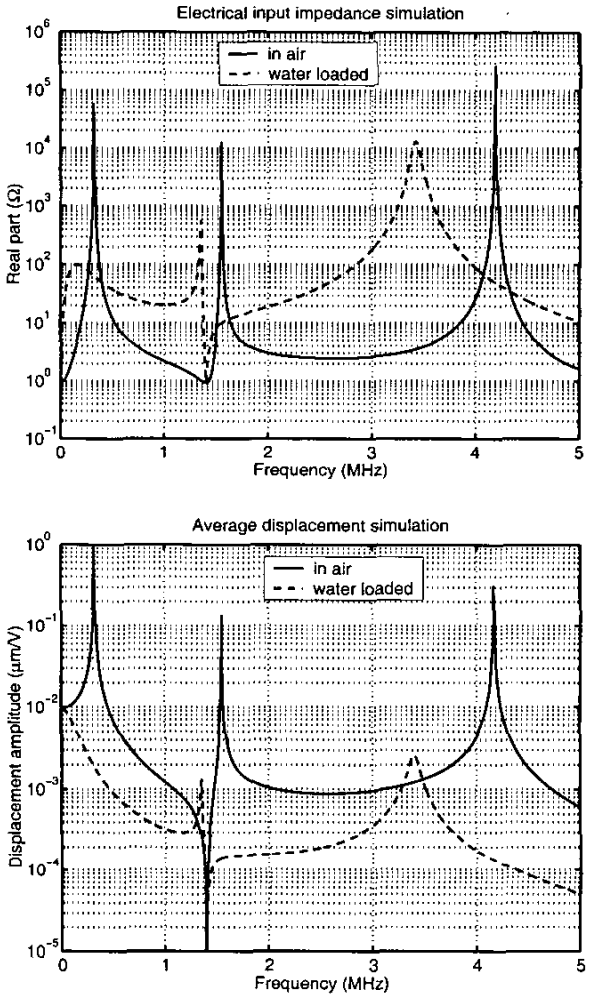

Fig. 16. Type II micromachined flextensional transducer simulations for a single element (Device E).

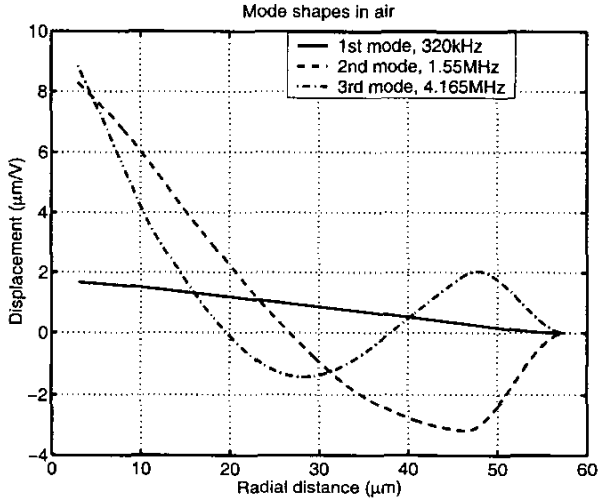

Fig. 17. Type II micromachined flextensional transducer simulations for a single element (Device E).

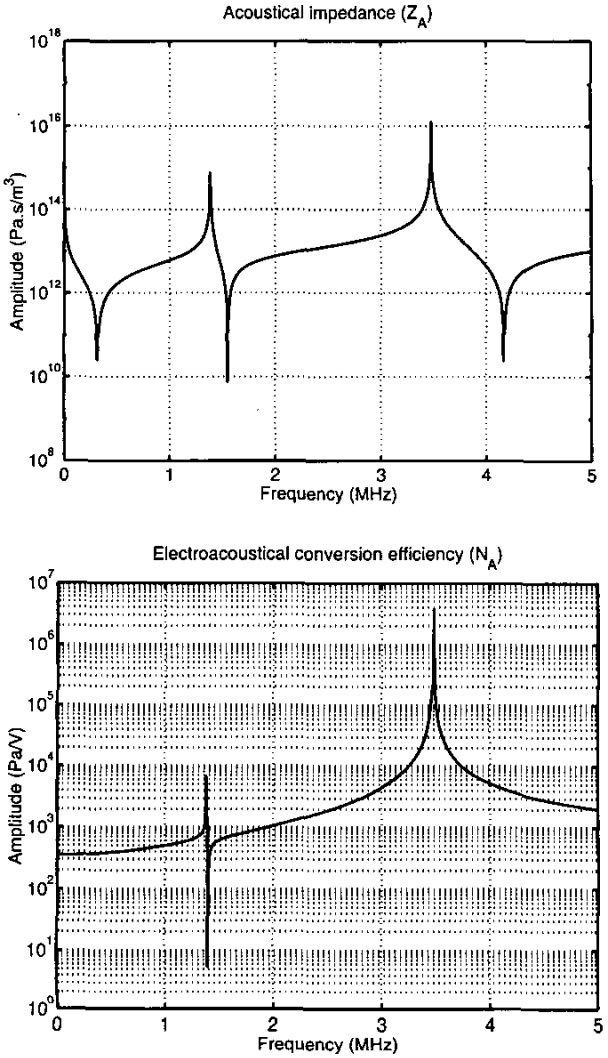

Fig. 18. Type II micromachined flextensional transducer simulations for a single element (Device E).

In the previous experiments, a low noise amplifier with a gain of 25 (28 dB) was used to amplify the received signal at the Type II device. Fig. 15 presents the real parts of the electrical input impedance of this Type II device for air-, water-, and isopropyl alcohol- (IPA-) loaded cases. As shown in Fig. 15, the resonances shift down in frequency and become relatively broadband (25%) when the device is loaded with a fluid. The shift in resonance for the water-loaded transducer is more than that for the IPA-loaded transducer because the acoustic impedance of water is larger than that of IPA. Another important point in Fig. 15 is the fact that the quality factor for the third resonance for fluid-loaded transducers is still relatively high, and this is because the third mode has relatively small coupling to the surrounding medium. This can be easily seen from the simulated electrical input impedance, average displacement, and mode shapes shown in Fig. 16 and 17. As a result, one can say that some resonant modes are suitable for ultrasound transducer applications, such as imaging, nondestructive evaluation, etc., and some resonant modes are suitable for fluid ejection applications caused by reduced acoustic coupling to the surrounding medium, but still large displacement. Finally, the acoustical impedance (Z_A) and electro-acoustical conversion efficiency (N_A) of the previous device are given in Fig. 18.

V. Conclusion

In summary, we have developed a novel ultrasonic transducer that is silicon micromachined into two-dimensional arrays. The individual array element is based on a variation of a flextensional transducer. The transducer design was optimized initially using finite element analysis, but later using the model developed in Perçin *et al.* [18], and the ultrasonic transmission was demonstrated in air and water.

Acknowledgment

This research was conducted during G. Perçin's Ph.D. study at Stanford University.

References

[1] J. J. Bernstein, S. L. Finberg, K. Houston, L. C. Niles, H. D. Chen, L. E. Cross, K. K. Li, and K. Udayakumar, "Micromachined high frequency ferroelectric sonar transducers," *IEEE Trans. Ultrason., Ferroelect., Freq. Contr.*, vol. 44, no. 5, pp. 960–969, Sep. 1997.

[2] J. Bernstein, K. Houston, L. Niles, S. Finberg, H. Chen, L. E. Cross, K. Li, and K. Udayakumar, "Micromachined ferroelectric transducers for acoustic imaging," in *Proc. Transducers '97*, pp. 421–424, 1997.

[3] Y. Takeuchi and T. Nanataki, "Method of producing piezoelectric/electrostrictive film element," US Patent No. 5,774,961, July 7, 1998.

[4] C. P. Germano, "Flexure mode piezoelectric transducers," *IEEE Trans. Audio Electroacoust.*, vol. AU-19, pp. 6–12, Mar. 1973.

[5] W. J. Denkmann, R. E. Nickell, and D. C. Stickler, "Analysis of structural-acoustic interactions in metal-ceramic transducers," *IEEE Trans. Audio Electroacoust.*, vol. AU-21, no. 4, pp. 317–324, Aug. 1973.

[6] A. M. Allaverdiev, N. B. Akhmedov, and T. D. Shermergor, "Coupled flexural-shear oscillations of stepwise-layered piezoceramic disk transducers," *Sov. Appl. Mech.*, vol. 23, pp. 465–471, May 1987.

[7] M. E. Vassergiser, A. N. Vinnichenko, and A. G. Dorosh, "Calculation and investigation of flexural-mode piezoelectric disk transducers on a passive substrate in reception and radiation," *Sov. Phys. Acoust.*, vol. 38, no. 6, pp. 558–561, Nov.-Dec. 1992.

[8] Y. T. Antonyak and M. E. Vassergiser, "Calculation of the characteristics of a membrane-type flexural-mode piezoelectric transducer," *Sov. Phys. Acoust.*, vol. 28, no. 3, pp. 176–180, May-Jun. 1982.

[9] É. S. Brailov and M. E. Vassergiser, "Estimation of the characteristics of a disk-shaped flexural-mode bimorph cell," *Sov. Phys. Acoust.*, vol. 26, no. 4, pp. 325–328, Jul.-Aug. 1980.

[10] N. T. Adelman and Y. Stavsky, "Flexural-extensional behavior of composite piezoelectric circular plates," *J. Acoust. Soc. Amer.*, vol. 67, no. 3, pp. 819–822, Mar. 1980.

[11] H. Okada, M. Kurosawa, S. Ueha, and M. Masuda, "New airborne ultrasonic transducer with high output sound pressure

level," *Jpn. J. Appl. Phys.*, pt. 1, vol. 33, no. 5B, pp. 3040–3044, May 1994.
[12] B. S. Aronov and L. B. Nikitin, "Calculation of the flexural modes of piezoceramic plates," *Sov. Phys. Acoust.*, vol. 27, no. 5, pp. 382–387, Sep.-Oct. 1981.
[13] B. S. Aronov and G. K. Skrebnev, "Effect of the attachment conditions of the piezoceramic plates on the parameters of circular laminated electromechanical transducers," *Sov. Phys. Acoust.*, vol. 29, no. 2, pp. 89–92, Mar.-Apr. 1983.
[14] F. J. Rosato, "Lagrange equations applied to flexural mode transducers," *J. Acoust. Soc. Amer.*, vol. 57, no. 6, pp. 1397–1401, Jun. 1975.
[15] J. B. Greenberg and Y. Stavsky, "Flexural vibrations of certain full and annular composite orthotropic plates," *J. Acoust. Soc. Amer.*, vol. 66, no. 2, pp. 501–508, Aug. 1979.
[16] Y. Stavsky and R. Loewy, "Axisymmetric vibrations of isotropic composite circular plates," *J. Acoust. Soc. Amer.*, vol. 49, no. 5, pt. 1, pp. 1542–1550, May 1971.
[17] A. J. Rudgers, "Acoustical behavior of thick, composite, fluid-loaded plates, calculated using Timoshenko-Mindlin plate theory," Naval Research Laboratory, Washington, D.C., Rep. no. 8317, Nov. 16, 1979.
[18] G. Perçin and B. T. Khuri-Yakub, "Piezoelectrically actuated flextensional micromachined ultrasound transducers—I: Theory," *IEEE Trans. Ultrason., Ferroelect., Freq. Contr.*, vol. 49, no. 4, pp. 573–584, May 2002.
[19] G. Perçin, L. Levin, and B. T. Khuri-Yakub, "Piezoelectrically actuated droplet ejector," *Rev. Sci. Instrum.*, vol. 68, no. 12, pp. 4561–4563, Dec. 1997.
[20] G. Perçin, T. S. Lundgren, and B. T. Khuri-Yakub, "Controlled ink-jet printing and deposition of organic polymers and solid-particles," *Appl. Phys. Lett.*, vol. 73, no. 16, pp. 2375–2377, Oct. 19, 1998.
[21] G. Perçin, A. Atalar, F. L. Degertekin, and B. T. Khuri-Yakub, "Micromachined two dimensional array piezoelectrically actuated transducers," *Appl. Phys. Lett.*, vol. 72, no. 11, pp. 1397–1399, Mar. 16, 1998.
[22] G. Perçin and B. T. Khuri-Yakub, "Micromachined 2-D array piezoelectrically actuated flextensional transducers," in *Proc. 1997 IEEE Int. Ultrason. Symp.*, pp. 959–962.
[23] ——, "Piezoelectrically actuated flextensional micromachined ultrasound droplet ejectors," *IEEE Trans. Ultrason., Ferroelect., Freq. Contr.*, to be published.

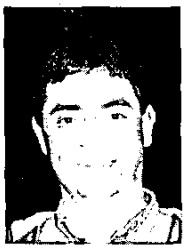

Gökhan Perçin (S'92–M'00) was born in Ezine, Çanakkale, Turkey. He received the B.S. degree in electrical and electronics engineering from Bilkent University, Ankara, Turkey in 1994. He received the M.S. degree in electrical engineering in 1996 and the Ph.D. degree in electrical engineering with minor subject in engineering-economic systems and operations research in 2002, both from Stanford University, California. He worked in Numerical Technologies, Inc., San Jose, California, as a senior software engineer to develop optical microlithography software. He is cofounder, president, and chief technical officer of ADEPTIENT, Los Altos, California. He has years of experience in the areas of fluid ejection, microfluidics, micromachining, micromachined electromechanical systems, ultrasonic actuators, ultrasound transducers, biomedical imaging, software development, sensors, and actuators. Dr. Perçin is a member of IEEE, IEEE Ultrasonics, Ferroelectrics, and Frequency Control Society, IEEE Electron Devices Society, the Electrochemical Society, and American Vacuum Society. His personal interests include Sufism, the Bektashi Order of Dervishes, photography, swimming, hiking, gourmet cooking, and collecting coins and stamps.

Butrus T. Khuri-Yakub (S'70–S'73–M'76–SM'87–F'95) was born in Beirut, Lebanon. He received the B.S. degree in 1970 from the American University of Beirut, the M.S. degree in 1972 from Dartmouth College, and the Ph.D. degree in 1975 from Stanford University, all in electrical engineering. He joined the research staff at the E. L. Ginzton Laboratory of Stanford University in 1976 as a research associate. He was promoted to Senior Research Associate in 1978 and to Professor of Electrical Engineering (Research) in 1982. He has served on many university committees in the School of Engineering and the Department of Electrical Engineering.

Presently, he is the Deputy Director of the E. L. Ginzton Laboratory. Professor Khuri-Yakub has been teaching both at the graduate and undergraduate levels for over 15 years, and his current research interests include in situ acoustic sensors (temperature, film thickness, resist cure, etc.) for monitoring and control of integrated circuits manufacturing processes, micromachining silicon to make acoustic materials and devices such as airborne and water immersion ultrasonic transducers and arrays, and fluid ejectors, and the field of ultrasonic nondestructive evaluation and acoustic imaging and microscopy.

Professor Khuri-Yakub is a fellow of the IEEE, a senior member of the Acoustical Society of America, and a member of Tau Beta Pi. He is Associate Editor of *Research in Nondestructive Evaluation*, a journal of the American Society for Nondestructive Testing. Professor Khuri-Yakub has authored over 300 publications and has been principal inventor or co-inventor of 52 issued patents. He received the Stanford University School of Engineering Distinguished Advisor Award (June 1987) and the Medal of the City of Bordeaux for contributions to NDE (1983).